Predicting the pressure dependence of the viscosity of 2,2,4-trimethylhexane using the SAFT coarse-grained force field

Lingru Zheng [a], J.P. Martin Trusler [a], Fernando Bresme [b], Erich A. Müller [a,*]

a) Department of Chemical Engineering, Imperial College London, U.K.
b) Department of Chemistry, Imperial College London, U.K.

Abstract

This work is framed within AIChE's 10th Industrial Fluid Properties Simulation Challenge, with the aim of assessing the capability of molecular simulation methods and force fields to accurately predict the pressure dependence of the shear viscosity of 2,2,4-trimethylhexane at 293.15 K (20 °C) at pressures up to 1 GPa. In our entry for the challenge, we employ coarse-grained intermolecular models parametrized via a top-down technique where an accurate equation of state is used to link the experimentally-observed macroscopic volumetric properties of fluids to the force-field parameters. The state-of-the-art version of the statistical associating fluid theory (SAFT) for potentials of variable range as reformulated in the Mie incarnation is employed here. The potentials are used as predicted by the theory, with no fitting to viscosity data. Viscosities are calculated by molecular dynamics (MD) employing two independent methods; an equilibrium-based procedure based on the analysis of the pressure fluctuations through a Green-Kubo formulation and a non-equilibrium method where periodic perturbations of the boundary conditions are employed to simulate experimental shear stress conditions. There is an indication that, at higher pressures, the model predicts a solid phase (freezing) which we believe to be an artefact of the simplified molecular geometry used in the modelling. A comparison (made after disclosure of the experimental data) show that the model consistently underpredicts the viscosity by about 30%, but follows the pressure dependency accurately.

1. Introduction

This work describes a submission to AIChE's 10th Industrial Fluid Properties Simulation Challenge [1], which was focused on assessing the capability of molecular simulation methods and force fields to accurately predict the pressure dependence of the shear viscosity of 2,2,4-trimethylhexane at 293.15 K (20 °C) at pressures up to 1 GPa. Viscosity calculations using standard molecular modelling tools have become routine [2]. While the "go-to" force field for these simulations is one of the many atomistic or united atom formulations (the reader is referred to other articles in this special issue), our interest was to probe the capabilities of coarse-grained models to predict viscosity, in particular models based on the Mie force fields which provide for an additional parameter (apart from the usual length and energy scales) which could be fine-tuned to provide for the description of transport properties alongside the volumetric properties for which they are usually optimized.

* Author to whom correspondence should be addressed (e.muller@imperial.ac.uk)

2. Methods

2.1.SAFT-γ CG Coarse graining methodology

For this challenge, we have employed the SAFT-γ CG force fields [3]. These are based on the Mie intermolecular potential, $u(r)$, which can be represented as

$$u(r) = C\varepsilon\left[\left(\frac{\sigma}{r}\right)^{\lambda} - \left(\frac{\sigma}{r}\right)^{6}\right] \quad (1)$$

$$C = \left(\frac{\lambda}{\lambda - 6}\right)\left(\frac{\lambda}{6}\right)^{6/(\lambda-6)} \quad (2)$$

In this equation, r is the centre-to-centre distance between two spherical isotropic segments, λ is a parameter that controls the steepness of the repulsion and the overall shape and range of the potential, σ is the average scale length of the spherical segments or beads, and ε represents the maximum depth of the potential well.

The above model parameters (σ, ε, λ) are estimated by adopting the "top-down" approach, where the parameters of the corresponding analytical equation of state (SAFT-VR-Mie) [4] are fitted to a range of experimental macroscopic properties, commonly include: vapour pressure, subcooled and supercritical densities. The crux of the methodology is that the equation of state parameters can be directly employed in molecular simulations, thanks to the one-to-one correspondence between the theory and the underlying models. SAFT force fields have been successful in describing thermophysical [5] interfacial [6,7], confined fluid [8] and transport properties [9,10] of a wide range of fluids and mixtures [11,12] including polymers [13].

Alternatively, if experimental data is unavailable, an estimation of the model parameters can be obtained from corresponding states correlations [14] for linear chain fluids and this has been implemented as a web tool to provide parameters for thousands of molecular fluids [15]. The method has recently been extended to produce parameters for planar ring compounds [16], wherein an additional parameter χ is included to take into account a ring structure at the level of the reference potential. We use this short-cut method, based on the corresponding states principle of the Mie fluids [17] to find explicit relationships between the molecular parameters and a reduced set of macroscopic volumetric properties. The procedure is detailed in references [14] and [16] but is detailed here for the case of 2,2,4-trimethylhexane.

Following the above procedure, the force field parameters for 2,2,4-trimethylhexane can be derived as follows. First, we obtain the Pitzer's acentric factor ω, from its definition:

$$\omega = -\log_{10}\left(\frac{P^{sat}\big|_{T_r=0.7}}{P_c}\right) \quad (3)$$

where T_c and P_c are the critical temperature and pressure respectively. The required saturated vapour pressure, P^{sat}, evaluated at a reduced temperature $T_r = T/T_c = 0.7$ can be estimated from an Antoine equation. Parameters for the Antoine correlation and the critical constants are taken from recommended values of the Dechema database [18]. Once a value of the acentric factor is available, the value of λ can be obtained directly via a Padé series [16]:

$$\lambda = \frac{\sum a_i \omega^i}{1 + \sum b_i \omega^i} \quad (4)$$

The repulsive exponent in Eq. (1) controls the shape of the potential, and as such, it is natural to relate it to the Pitzer's acentric factor, ω, a measure of the deviation of the vapour pressure curve of a fluid as compared to that of a noble gas. The value of λ takes into account the non-conformality of the fluid. Furthermore, this non-conformality gives rise to a whole family of fluids, called generally Mie fluids, each with a unique characteristic fluid range [17]. The different Mie fluids can be characterised by the van der Waals constant, α_{vdW}, defined and calculated as [17]

$$\alpha_{vdW} = \frac{1}{\varepsilon\sigma^3}\int_{\sigma}^{\infty} u(r) r^2 \, dr = C\left[\frac{1}{3} - \left(\frac{1}{\lambda - 3}\right)\right] \quad (5)$$

For a specific fluid with a given value of α_{vdW}, the critical and phase behaviour properties can be uniquely expressed in reduced units [16]:

$$T_c^* = \frac{\sum c_i \alpha_{vdW}^i}{1 + \sum d_i \alpha_{vdW}^i} \qquad \rho^*\big|_{T_r=0.7} = \frac{\sum e_i \alpha_{vdW}^i}{1 + \sum f_i \alpha_{vdW}^i} \quad (6)$$

The values of coefficients a_i to f_i in Eq. (4), and (6) are tabulated in [16] and are related to the specific geometry of the model. In this case, we assume the structure can be represented by three connected beads (corresponding to m_s = 3) in a triangular planar configuration. An illustration is shown in Fig.1.

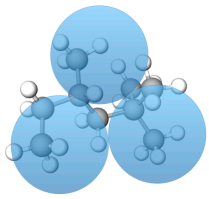


Figure 1: Coarse grained model for 2,2,4-trimethylhexane, formed of three equal tangent Mie beads in an equilateral configuration. A cartoon of an atomistic model of the molecule is superimposed for comparison.

Finally, ε and σ can be calculated based on the definition of dimensionless temperature and density:

$$\varepsilon / k_B = \frac{T_c}{T_c^*} \quad , \quad \sigma^3 = \frac{\rho^*\big|_{T_r=0.7}}{\rho\big|_{T_r=0.7}} \quad (7)$$

To calculate σ, it is necessary to know the density at $T_r = T / T_c = 0.7$, the so-called normal density. We fit a second polynomial to experimentally reported densities in a range of temperatures close to the target (400K) temperature to extract this value from the density data provided by DECHEMA [18].

Table 1 Experimental data to employed to generate force field parameters for 2,2,4-trimethylhexane. T_c is the critical temperature, ω is the acentric factor and $\rho|_{T_r=0.7}$ is the normal density at 0.7 reduced temperature.

T_c [K]	ω	$\rho\big\|_{T_r=0.7}$ [kg.m^{-3}]
573.65	0.3493	615.097

We summarise the experimental data used for parameter fitting in Table 1 and the final force field parameters in Table 2. In this case, the molecule is assumed to adopt a planar equilateral ring structure, so no bond bending potential is enforced. No fitting is made of the intramolecular potential, and in absence of any further information a stiff (or rigid) bond is assumed between the centers of the molecules with a center-to-center distance equal to σ in an equilateral triangular configuration.

Table 2 SAFT-γ CG Mie force field parameters for 2,2,4-trimethylhexane. m_S is the number of CG beads in each molecule, σ is the bead size parameter, ε is the energy parameter, where k_B is Boltzmann's constant, and λ is the repulsive exponent. The beads in a molecule are held together by rigid bonds with a center-to-center distance equal to σ.

m_s	σ [nm]	ε/k_B [K]	λ
3	0.4417	300.134	14.408

We use the previously determined SAFT-γ Mie forcefields in MD simulations to predict shear viscosities without any further fitting. Two algorithms are used, a pressure fluctuation method based on the Green-Kubo formulation, as well as a non-equilibrium method based on periodic perturbations.

2.2.Equilibrium pressure fluctuation method

We use the Green-Kubo (GK) methodology [19,20] which links the shear viscosity to the equilibrium correlation of the pressure fluctuations:

$$\eta = \frac{V}{k_B T}\int_0^\infty \left\langle P_{ij}(t)P_{ij}(t+\tau)\right\rangle_\tau d\tau \quad (8)$$

where V is the system volume, and P_{ij} are the off-diagonal elements of the pressure tensor, *i.e.* $i \neq j$; their values being recorded during MD simulations as a function of time t. In Eq. (8), the integrand represents the autocorrelation function (ACF) of the components of the pressure tensor with respect to a time delay τ .

2.3.Non-equilibrium molecular dynamics (NEMD) method

To implement a non-equilibrium method, we employ periodic perturbations where an external force is applied to the system and the response to this perturbation is monitored. To comply with MD simulations, where velocity is defined periodically, an external force can be added as an acceleration term to the macroscopic Navier-Stokes equations using a cosine function $\mathcal{A}\cos(k_z z)$, assuming it has only the x-component (flow direction) and it is a function of z only. Here $k_z = 2\pi / l_z$ is the wave vector and l_z is the box length in the z direction direction (perpendicular to the induced flow). Hence, the velocity profile U_x can be written as:

$$U_x(t,z) = \mathcal{A}\frac{\rho}{k_z^2 \eta}\left(1 - e^{-t/\tau_H}\right)\cos(k_z z) \quad (9)$$

Where $\rho/k_z^2\eta$ can be written as τ_H, the hydraulic time constant, which represents the relaxation time of the plane waves travelling in the fluid. In MD, acceleration can be added to each step, hence an average of $\mathcal{A}(\rho/k_z^2\eta)$ can be computed to give the value of η [21].

3. Simulation details

All simulations were performed with the GROMACS 5.1.3 suite [22] with no modifications and based on classical Molecular Dynamics algorithms. The process flow of the simulations strategy is summarized in the SI. To calculate the system's viscosity, 3000 2,2,4-trimethylhexane model molecules are placed randomly in a cubic box and the system is compressed under the *NPT* ensemble to reach the desired pressure and temperature. Equilibrium can be achieved within the first few picoseconds for systems with pressures at or below 400 MPa whilst at higher pressures the system starts to solidify, and the equilibration process slows down significantly. From a group of separate tests running *NPT* up to 10 micro seconds, we observed various degrees of solid-fluid equilibrium at the higher pressures (see discussion in section 4.1).

For each system, to ensure the configuration we picked for subsequent simulations would have a system volume corresponding to the specified pressure, we ran 10 ns in the *NPT* ensemble to ensure equilibration of the system and further 30 ns as the production run; from the 30 ns-trajectory we computed the average system volume. Afterwards, a frame with box size smaller than the average is chosen from the trajectory and we manually change its box size to the average. Using the selected frames as the starting points, we continued the simulation under the *NVT* ensemble for another 10ns to equilibrate the system. The configurations yield from above procedure were then used as the initial equilibrated boxes for subsequent equilibrium and non-equilibrium MD simulations carried out in separate paths to compute the viscosity. For high pressure systems, we searched for these configurations when no solids are present (by examining both the radial distribution functions and visual inspection). Throughout the subsequent equilibrium and non-equilibrium MD simulations, the Nosé-Hoover thermostat and the isotropic Berendsen barostat are chosen for temperature and pressure control, respectively, both with a 2ps time constant. Other choices of thermostats were explored, but the results are invariant to the choice. The cutoff of the potential is set at 2 nm (roughly 4.5 σ) which is deemed to be sufficiently large as to be able to neglect any effects due to the truncation of the force field: no long-range corrections have been applied.

The equilibrium MD (GK) path involves running the simulation under an *NVT* ensemble with a 2fs time step, and the pressure values are recorded for every time step. To obtain sensible statistics, we carry out the simulation 10 times each for 10 ns at $P \leq 400$ MPa, and for 20 ns at $P > 400$ MPa. Since each simulation generates three independent pressure component trajectories (P_{xy}, P_{xz} and P_{yz}), there are in total of 30 trajectories to average for each state point.

To implement the GK in practice, the integrand in eq. (8) is solved numerically from the beginning of the simulation taking the natural intervals provided by an MD simulation from 0

to n_{max} -1 at each discrete time step, where n_{max} is the maximum number of recorded steps. To mitigate the effects of the statistical uncertainty we remove any invariant part of the pressure components that have been built-up during the simulation, employing the normalised autocorrelation expression:

$$\left\langle P_{ij}(t)P_{ij}(t+\tau)\right\rangle_{\tau} = \frac{1}{n_{\max}}\sum_{\tau=0}^{\tau_{\max}}\left(P_{ij}(t)-\overline{P_{ij}}\right)\left(P_{ij}(t+\tau)-\overline{P_{ij}}\right) \quad (10)$$

where $ij = xy, xz, yz$ and $\overline{P_{ij}}$ is the mean value of all the recorded values of the pressure components. A drawback of the (GK) pressure fluctuation algorithm is the difficulty of collecting good statistics, due to large fluctuations of the recorded pressure [23] and the methods used to collect the statistics. A key point in the numerical procedure is the specification of the time deemed to be sufficient to assume decorrelation in the autocorrelation function, *i.e.* the "infinite" time. The details of the choosing of this time are given in the SI. A simulation taken after there is a drop in the ACF will essentially just accumulate statistical noise that will eventually obscure the underlying value of viscosity.

Inspired by Maginn et al.'s suggested strategies [2, 21] we perform multiple re-runs of the simulation (with different starting points) and fit the running integral of the average viscosity to a double exponential function given as Eq. (11) from which the resulting viscosity is read out at a simulation time corresponding to the decay of the ACF. The details of the procedure and a sample calculation are given in the SI.

$$\eta(t) = A\alpha\tau_1(1-e^{-t/\tau_1}) + A(1-\alpha)\tau_2(1-e^{-t/\tau_2}) \quad (11)$$

The expected standard deviation is calculated at this value of time by fitting a power law equation:

$$\sigma_{\eta}^{GK}(t) = Bt^{b} \quad (12)\,,$$

to the standard deviation of the viscosities (σ_{η}^{GK}) versus correlation time (t). Here, and in equation (11), A, B, b, α, τ_1 and τ_2 are empirical fitting parameters. In the SI we describe a numerical example.

For the non-equilibrium MD (NEMD) procedure, the selected configuration file is simulated under the *NVT* ensemble for 2 ns at least 6 different cos-acceleration amplitudes, each for three times. The amplitudes are often chosen to be lower than 0.1 nm.ps^{-2} to avoid shear thinning or thickening. The viscosity is output as "1/viscosity" via the `g_energy` subroutine from GROMACS. We apply a weighted linear fit to the data points on the viscosity versus acceleration graph, with the weight inversely proportional to the statistical viscosity error σ_{η}^{NEMD} [21]

$$\sigma_{\eta}^{\mathrm{NEMD}} = \frac{2}{s_{\max}}\sqrt{\frac{k_{\mathrm{B}}T\eta}{Vt_{\mathrm{a}}}} \text{ where } \quad s_{\max} = \mathcal{A}\frac{\rho}{\eta k} \quad (13)$$

Here, t_{a} is the time over which the average velocity is determined. $s_{\max}$ is the maximum shear rate and $\mathcal{A}$ is the value of acceleration in nm.ps^{-2}. In the SI we describe a numerical example.

4. Results

4.1 Solid phases

Upon coarse-graining (CG) the n-alkane models, one loses much of the detail of the atomic structure: on average three connected carbon atoms and their corresponding hydrogens are all lumped into a spherical bead, which itself is connected in a regular configuration to other similar beads. Clearly, this low-resolution model is incapable of reproducing all the subtleties of molecular crystals. The SAFT CG models are based on a fitting of the liquid-vapor equilibrium properties (both densities and vapor pressures) guaranteeing that the parameters are a 'best-compromise' fit with information on the effective molecular size (through the density fits), the width-to-length ratio (through the value of m_s, the number of beads in the model), and the effective average non-bonding energy and potential shape (through the fits to the vapor pressure). Another relevant reference to this point is the article by Maginn *et al*. [24] where the differences in property predictions due to the force field nature and parametrization were investigated by the comparison of seven different CO_2 models (two single-site models, three rigid three-site models, and two fully flexible three-site models) and three different CH_4 models (two single-site models and one fully flexible five-site model). In both cases, the SAFT CG models fared similarly to more refined all-atom models, despite the fact that the comparison was made with what we consider to be a sub-optimal CO_2 model.

One noticeable aspect in our model is its unphysical regularity and symmetry, *c.f.* Fig. (1). The molecular model coarse-grains the geometry into an overly simplified triad of tangent spheres. This has an important consequence that it will induce the premature freezing of the fluid in an FCC-like crystal (Fig 2) . We have detected this to happen at pressures of 400-500 MPa, although no effort was made to pin-point the transition pressure (see Fig. 3). We believe the incipient formation of a solid phase made our simulations unreliable above 400 MPa, as we observe nuclei of solids forming during the simulation. This nucleation process is slow and only perceptible during very long simulations.

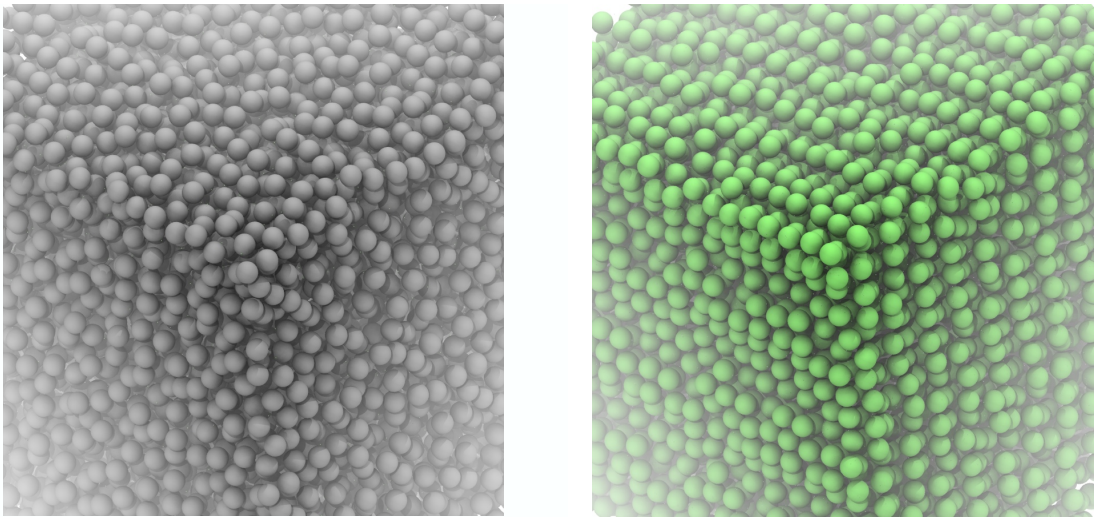


Figure 2. Snapshots of equilibrated states at 150 MPa (left) and 500 MPa (right) seen from a corner of the simulation cell. The structure at the right suggests an ordered structure typical of a solid. These are examples taken from very long simulation runs (> 10 μs) on a smaller system (300 molecules) where we expect the system to have equilibrated to the most stable phase.

4.2 Density

We present in Fig. 3 the equilibrium density of the system as a function of the pressure. We see how at 400 MPa (and higher pressures), the system exhibits a transition to a solid phase. As discussed above, we did not perform any free energy or stability analysis of the coexisting phases and employed only the fluid phase to report results.

The SAFT model we employ has the uniqueness that for volumetric properties there is a link between the underlying equation of state and the simulation results. We have explored that parallelism in Fig. 3 and show a divergence between the simulated densities and the predicted equation of state results. At this point we do not know the reasons behind the lack of agreement between simulation and theory and will not speculate on its meaning.

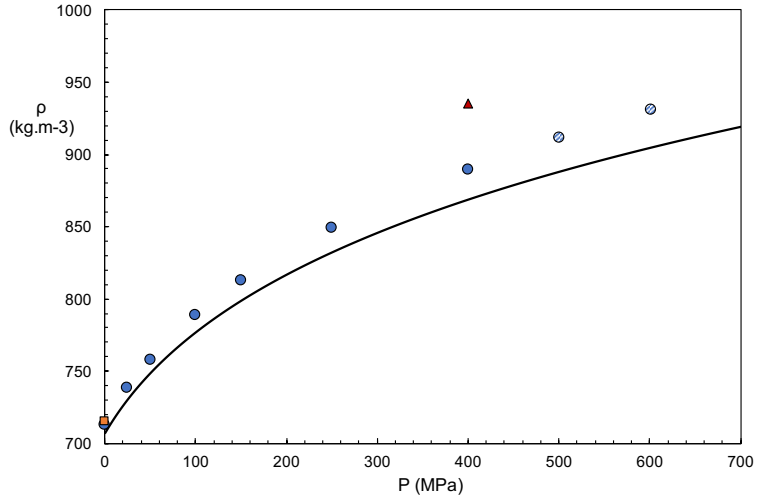


Figure 3. Density, ρ , of 2,2,4-trimethylhexane computed through MD at 293.15 K from 0.1 MPa to 600 MPa (blue circles) as compared to experimental value, ref. [18] (yellow square) and the corresponding result from the SAFT equation of state (line). Red triangle is a solid state obtained from MD. Hashed circles are presumed metastable liquids. Error bars are of the order or smaller than symbol size.

4.3 Shear viscosity

For a 2,2,4-trimethylhexane system, 3000 molecules are simulated at 293.15 K and pressures from 0.1 MPa up to 600 MPa. Simulation results are plotted in Fig. 4. The results are compared to an experimental point determined at ambient pressure and temperature reported in ref. [25] of η = 0.648 mPa·s, which suggests that at this condition the model is under-predicting the viscosity by about 40%. No attempt was made to adjust the model parameters to this value prior to the challenge.

The results from the equilibrium and non-equilibrium methods agree well amongst themselves. We do not report high-pressure viscosities as the system congealed at these conditions. The NEMD simulations allowed us to tentatively explore the fluid region, presumably because the shearing suppressed the nucleation, especially for shorter runs, however, long simulations inevitably produced solid nucleation sites which provided for simulation values which were orders of magnitude larger than those expected. The NEMD data point at 400 MPa is an outlier, presumably because of the influence of solid nuclei in the structures. After the disclosure of the experimental data we observed that indeed, neither the metastable liquids nor the mixed solid-fluid systems were representative of the actual fluid.

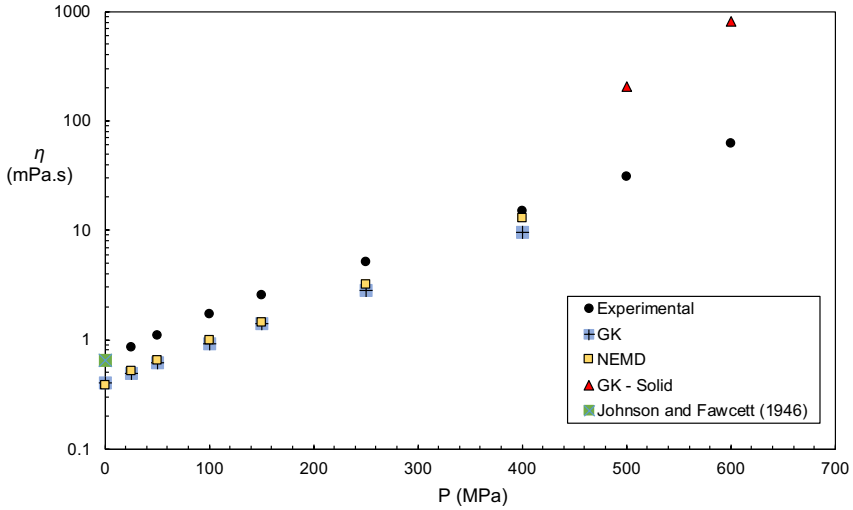


Figure 4. Shear viscosity of 2,2,4-trimethylhexane computed at 293.15 K from 0.1 MPa to 600 MPa using two different algorithms: equilibrium Green Kubo (GK) via pressure fluctuations (blue crosses) and periodic non-equilibrium molecular dynamics (NEMD) (yellow squares). The molecular model freezes prematurely (red triangle) at around 500 MPa and above, hence the viscosity data is not available at higher pressures. A known experimental point (green square) from ref. [25] is shown along with the disclosed experimental data [1] (black circles).

Table 2 Predicted shear viscosities, η, and corresponding error estimate, $\sigma_{\eta,}$ for 2,2,4-trimethylhexane computed at 293.15 K. The model solidifies prematurely at pressures higher than 400 MPa. Data points marked with a superscript (sol) correspond to state points which correspond to solids. An uncertainty of 30% is estimated for the state points at and below 150 MPa, 40% for state points at 250 through 400 MPa. Experimental (Expt.) data are the disclosed challenge benchmark results [1]. GK and NEMD correspond to the Green-Kubo and non-equilibrium molecular dynamics approaches respectively. Scaled results correspond to the GK values scaled with respect the low pressure experimental point.

	Expt.	GK		NEMD		Scaled
P (MPa)	η (cP)	η (mPa·s)	σ_η (mPa·s)	η (mPa·s)	σ_η (mPa·s)	η (mPa·s)
0.1	0.64	0.40	0.09	0.38	0.01	0.64
25	0.844	0.49	0.09	0.51	0.01	0.78
50	1.101	0.61	0.11	0.64	0.02	0.98
100	1.71	0.92	0.15	0.98	0.03	1.5
150	2.54	1.40	0.43	1.43	0.06	2.2
250	5.13	2.80	0.99	3.23	0.18	4.5
400	15	9.47	2.46	13	2	15
500	30.9	205^{sol}	167^{sol}	-	-	-
600	62.9	806^{sol}	378^{sol}	-	-	-

5. Final Comments

Simulations at lower pressures (< 400 MPa) proved to be of a rather routine nature, with the system behaving as expected and very clear trends provided in the estimation of the viscosities. Both the equilibrium (GK) and NEMD methods converged and produced results which are within each other's degree of uncertainty. However, the viscosity of the fluid increased by several decades as the different higher-pressure levels were explored, and while the coarse-grained model allowed us to access these states, the freezing of the underlying model precluded an accurate representation of the liquid state viscosities. For the state points reported, the viscosity of the CG model is consistently lower than the reported experimental values. A common explanation for this result is the assumption that by integrating out the atomistic features CG models are incapable of reproducing viscosities. Recent manuscripts challenge this vision [26,27], noting that appropriately parametrized CG models can correctly represent both volumetric and transport properties. If the results of our model are scaled to the low-pressure data point, the results of the Mie model become quantitative in nature, as the slope of both the simulation and the experiments agree (*c.f.* Table 2). This scaling procedure (in this case multiplying by $\eta/\eta_{ref} = 0.64/0.4$) is standard practice in thermophysical property modelling and correlation and is presented only to highlight a classical data fitting feedback procedure. We have not scaled the molecular parameters nor are claiming that the scaling has any physical meaning, but does suggest that other types of parametrizations would provide CG models that can be used to accurately calculate the viscosity of real fluids.

The proposed coarse-grained model suffers from deficiencies caused by it simplified nature. Specifically, its symmetry and regularity induces a premature solidification which we deem an artefact of the model, but might be avoided if other experimental (or *ab-initio*) information was used to refine the model geometry. Our models assumed a rigid bonding between the spheres. We have seen in our simulations that relaxing this rigidity does not seem to improve the predictions.

6. References

[1] http://fluidproperties.org/

[2] E. Maginn, R. Messerly, D. Carlson, D. Roe, and R. Elliott, Best Practices for Computing Transport Properties 1. Self-Diffusivity and Viscosity from Equilibrium Molecular Dynamics [Article v1.0], *LiveCoMS*, 1, 1–20, 2018.

[3] E. A. Müller and G. Jackson. Force-field parameters from the SAFT-γ equation of state for use in coarse-grained molecular simulations. *Annu. Rev. Chem. Biochem. Eng.*, 5:405– 427, 2014.

[4] T. Lafitte, A. Apostolakou, C. Avendaño, A. Galindo, C. S Adjiman, E. A Müller, and G. Jackson. Accurate statistical associating fluid theory for chain molecules formed from Mie segments. *J. Chem. Phys*, 139,154504, 2013

[5] C. Avendaño, T. Lafitte, A. Galindo, C. S Adjiman, G. Jackson, and E. A Müller. SAFT-γ force field for the simulation of molecular fluids. 1. a single-site coarse grained model of carbon dioxide. *J. Phys. Chem. B*, 115, 11154–11169, 2011.

[6] P. Morgado, O. Lobanova, E. A. Müller, G. Jackson, M. Almeida, and E. J. M. Filipe, SAFT-γ force field for the simulation of molecular fluids: 8. Hetero-segmented coarse-grained models of perfluoroalkylalkanes assessed with new vapour–liquid interfacial tension data, *Mol. Phys.*, 114, 2597–2614, 2016.
[7] C. Herdes, Å. Ervik, A. Mejía, and E. A. Müller, Prediction of the water/oil interfacial tension from molecular simulations using the coarse-grained SAFT-γ Mie force field," *Fluid Phase Equilibria*, 476, 9–15, 2018.
[8] C. Herdes, C. Petit, A. Mejía, and E. A. Müller, Combined Experimental, Theoretical, and Molecular Simulation Approach for the Description of the Fluid-Phase Behavior of Hydrocarbon Mixtures within Shale Rocks *Energy Fuels*, 32, 5750–5762, 2018.
[9] F. Jaeger, O. K. Matar, and E. A. Müller, Bulk viscosity of molecular fluids, *J Chem Phys*, 148, 174504–12, 2018.
[10] S. Shahruddin, G. Jiménez-Serratos, G. J. P. Britovsek, O. K. Matar, and E. A. Müller, Fluid-solid phase transition of n-alkane mixtures: Coarse-grained molecular dynamics simulations and diffusion-ordered spectroscopy nuclear magnetic resonance, *Sci Rep*, 9, 1–9, 2019.
[11] C. Herdes, T. S. Totton, and E. A. Müller, "Coarse grained force field for the molecular simulation of natural gases and condensates," *Fluid Phase Equilibria*, 406, 91–100, 2015.
[12] O. Lobanova, A. Mejía, G. Jackson, and E. A. Müller, SAFT-γ force field for the simulation of molecular fluids 6: Binary and ternary mixtures comprising water, carbon dioxide, and n-alkanes, *J. Chem. Thermodyn.*, 93, 320–336, 2016.
[13] G. Jiménez-Serratos, C. Herdes, A. J. Haslam, G. Jackson, and E. A. Müller, Group Contribution Coarse-Grained Molecular Simulations of Polystyrene Melts and Polystyrene Solutions in Alkanes Using the SAFT-γ Force Field, *Macromolecules*, 50, 4840–4853 (2017).
[14] A. Mejía, C. Herdes, and E. A. Müller. Force fields for coarse-grained molecular simulations from a corresponding states correlation. *Ind. Eng. Chem. Res.*, 53, 4131–4141, 2014.
[15] Å. Ervik, A. Mejía, and E. A. Müller. Bottled SAFT: a web app providing SAFT-γ Mie force field parameters for thousands of molecular fluids. *J. Chem. Inform. Model.*, 56, 1609–1614, 2016.
[16] E. A. Müller and A. Mejía. Extension of the SAFT-VR Mie EoS to model homonuclear rings and its parametrization based on the principle of corresponding states. *Langmuir*, 33,11518–11529, 2017
[17] N.S Ramrattan, C Avendaño, E.A. Müller, and A. Galindo. A corresponding-states framework for the description of the Mie family of intermolecular potentials. *Molecular Phys.*, 113, 932–947, 2015
[18] J. Gmehling, U. Onken, W. Arlt, et al. *Vapor-liquid equilibrium data collection*, volume1. Dechema Frankfurt am Main, 1979.
[19] M. S. Green. Markoff random processes and the statistical mechanics of time-dependent phenomena. ii. irreversible processes in fluids. *J. Chem. Phys.*, 22, 398–413, 1954.
[20] R. Kubo. Statistical-mechanical theory of irreversible processes. I. general theory and simple applications to magnetic and conduction problems. *J Phys. Soc. Japan*, 12(6):570–586, 1957.
[21] B. Hess Determining the shear viscosity of model liquids from molecular dynamics simulations. *J. Chem. Phys.*, 116, 209–217, 2002.
[22] Abraham, et al. GROMACS: High performance molecular simulations through multi-level parallelism from laptops to supercomputers *Software X* 1-2 19-25, 2015
[23] Y. Zhang, A. Otani, and E. J Maginn. Reliable viscosity calculation from equilibrium molecular dynamics simulations: a time decomposition method. *J. Chem. Theory Comput.*, 11, 3537–3546, 2015
[24] C. G. Aimoli, E. J. Maginn, and C. R. A. Abreu, Transport properties of carbon dioxide and methane from molecular dynamics simulations. *J Chem. Phys*, 141, 134101, 2014
[25] G.C. Johnson, F.S. Fawcett, Inter-polymerization of Isobutene and 2-methyl-2butene using alumina-silica Catalyst. Composition of the Hydrogenated Nonenes. *J. Amer. Chem. Soc.* 68, 1417, 1946
[26] H. Hoang, S. Delage-Santacreu, and G. Galliero, Simultaneous Description of Equilibrium, Interfacial, and Transport Properties of Fluids Using a Mie Chain Coarse-Grained Force Field, *Ind. Eng. Chem. Res.*, 56, 9213–9226, 2017.
[27] S. Rahman, O. Lobanova, G. Jiménez-Serratos, C. Braga, V. Raptis, E. A. Müller, G. Jackson, C. Avendaño, and A. Galindo, SAFT-γ Force Field for the Simulation of Molecular Fluids. 5. Hetero- Group Coarse-Grained Models of Linear Alkanes and the Importance of Intramolecular Interactions. *J. Phys. Chem. B*, 122, 9161–9177, 2018.